OPEN

PRS GLOBAL OPEN

ORIGINAL ARTICLE

Technology

Clinical Application to Improve the "Depth Perception Problem" by Combining Augmented Reality and a 3D Printing Model

Misato Katayama, MD
Daisuke Mitsuno, MD, PhD
Koichi Ueda, MD, PhD

Background: In our experience with intraoperative evaluation and educational application of augmented reality technology, an illusion of depth has been a major problem. To improve this depth perception problem, we conducted two experiments combining various three-dimensional models and holograms and the observation angles using an augmented reality device.

Methods: In experiment 1, when observing holograms projected on the surface layer of the model (bone model) or holograms projected on a layer deeper than the model (body surface model), the observer's first impression regarding which model made it easier to understand positional relationships was investigated. In experiment 2, to achieve a more quantitative evaluation, the observer was asked to measure the distance between two specific points on the surface and deep layers from two angles in each of the above combinations. Statistical analysis was performed on the measurement error for this distance.

Results: In experiment 1, the three-dimensional positional relationships were easier to understand in the bone than in the body surface model. In experiment 2, there was not much difference in the measurement error under either condition, which was not large enough to cause a misunderstanding of the depth relationship between the surface and deep layers.

Conclusions: Any combination can be used for preoperative examinations and anatomical study purposes. In particular, projecting holograms on a deep model or observing positional relationships from not only the operator's viewpoint, but also multiple other angles is more desirable because it reduces confusion caused by the depth perception problem and improves understanding of anatomy. *(Plast Reconstr Surg Glob Open 2023; 11:e5071; doi: 10.1097/GOX.0000000000005071; Published online 23 June 2023.)*

INTRODUCTION

Augmented reality (AR)[1] is a new technology that seamlessly overlays computer-generated images onto the real world and combines them with real objects or scenes, and has received increasing attention in recent years. This technology is widely used in medical fields[2] such as surgery,[3,4] treatment,[5,6] examinations,[7] rehabilitation,[8] telemedicine,[9,10] and medical education.[11,12]

In our previous reports, we have shown that projecting holograms onto the operative field is useful for intraoperative evaluations[13] in a variety of cases. In some of these cases, three-dimensional (3D) models have been used for preoperative examination and the projection of holograms onto such models has also seemed to be effective. Therefore, we conceived the idea of projecting a hologram onto the model to increase its effectiveness for preoperative examination and educational use.[9,14]

A common use of AR in the surgical field is to project holograms of deep organ onto the surgical field. Accordingly, it is first assumed that holograms of deep

From the Department of Plastic and Reconstructive Surgery, Osaka Medical and Pharmaceutical University, Takatsuki City, Osaka, Japan.

Received for publication March 22, 2023; accepted April 28, 2023.

Presented in part at the 31st Research Council Meeting of the Japan Society of Plastic and Reconstructive Surgery, 2022, Okayama, Japan.

DOI: 10.1097/GOX.0000000000005071

Disclosure statements are at the end of this article, following the correspondence information.

Related Digital Media are available in the full-text version of the article on www.PRSGlobalOpen.com.

organs will be projected onto a body surface model. However, in this case, an illusion known as the depth perception problem (DPP)[15,16] arises in which a hologram located behind a real object appears to be in front of it because of occlusion on the display; this is a major challenge in the use of AR in the surgical field.[17,18]

On the other hand, projecting holograms of superficial organs (eg, blood vessels) onto a deeply situated bone model may also be effective for preoperative examinations and educational use. In such a case, theoretically, there is no DPP because the holograms are more superficial than the real object.

In addition, in the surgical field, the angles of observation are likely to be limited; therefore, in the present study, which utilized models, no restrictions were placed on the angles of observation, which may reduce DPP further.

In this study, we performed two experiments to investigate whether the DPP could be improved by adjusting the vertical relationships between the models and holograms and the observation angles.

Takeaways

Question: This study aims to solve the illusion of the depth perception problem (DPP). This issue is important when using augmented reality technology in the surgical field.

Findings: Two experiments using an augmented reality device and three-diemensional models showed that the DPP can be improved by adjusting the vertical relationship between the model and the hologram and the angle of observation.

Meaning: This method can be used for preoperative examinations and anatomical study purposes in surgery at very shallow depths between the skin and subcutaneous areas, such as in the field of plastic surgery.

MATERIALS AND METHODS

Work Flow

The AR device used was the HoloLens (Microsoft Corp., Redmond, Wash.), a head-mounted device capable of displaying stable virtual objects. Models and holograms were created based on 3D data of the same facial region extracted from the computed tomographic scan data of a patient with micrognathia. Three types of models were created: a bone model, a translucent body surface model, and an opaque body surface model. The holograms created were of the body surface, blood vessels, and bones. As a method for aligning the models and holograms, we used our originally developed application,[19] which aligns holograms based on three points on the surface of the real object. The following is a description of the method used to create the models and holograms (Fig. 1).

Processing of the 3D Data

Digital Imaging and Communication in Medicine (DICOM) data obtained from the computed tomographic scans were segmented into the body surface, blood vessels, and bones using free open-source software (3D Slicer; http://www.slicer.org), and converted into 3D data. These data were imported into free 3D data-editing software (Blender; Blender Foundation, Amsterdam, the Netherlands; www.blender.org) and processed into the 3D data required for models and holograms (this included removing unnecessary parts and reducing the overall data volume). At that time, two measurement points and three reference points for alignment were established. The measurement points were point a on the bone surface and point b on the body surface.

Creation of the Models

The 3D modeling devices used were FlashForge Guider II (FlashForge, Zhejiang, China) and Form2 (Formlabs, Kyoto, Japan), and the materials used were acrylonitrile-butadiene-styrene resin or ultraviolet (UV)-cured resin. For the body surface model, 3D data of the body surface extracted at a thickness of 1 mm was used. The translucent body surface model was made of clear UV-cured resin, and the opaque body surface model was made of acrylonitrile-butadiene-styrene resin.

Creation of the Holograms

In addition to the body surface, blood vessel, and bone data processed in Blender, Filmbox (.fbx) files including two measurement and three alignment reference points were imported into a free game engine (Unity; Unity Technologies, Copenhagen, Denmark) to create a hologram-viewing application for HoloLens.

Experiment 1

In experiment 1, when observing holograms projected on the surface layer of the model (bone model) or holograms projected on a layer deeper than the model (body surface model), the observer's first impression regarding which model made it easier to understand positional relationships was investigated. The holograms of blood vessels were projected onto each of the three models: a bone model, a translucent body surface model, and an opaque body surface model with alignment (Fig. 2). Then, 10 junior residents rated their first impression of whether they could grasp the 3D relationship between the holograms of the blood vessels and each model—that is, which was superficial or deep, on a three-point scale [1, "I could recognize it immediately after starting the observation"; 2, "I could recognize it after some time (without specifying the time required)"; and 3, "I couldn't recognize it"]. Trends in the evaluation results by model were then compared.

Experiment 2

In experiment 2, to achieve a more quantitative evaluation, the observer was asked to measure the distance between two specific points on the surface and deep layers from two angles in each of the above combinations. A hologram of the body surface was projected onto the bone model, and a hologram of the bone was projected onto the translucent body surface model. The distance

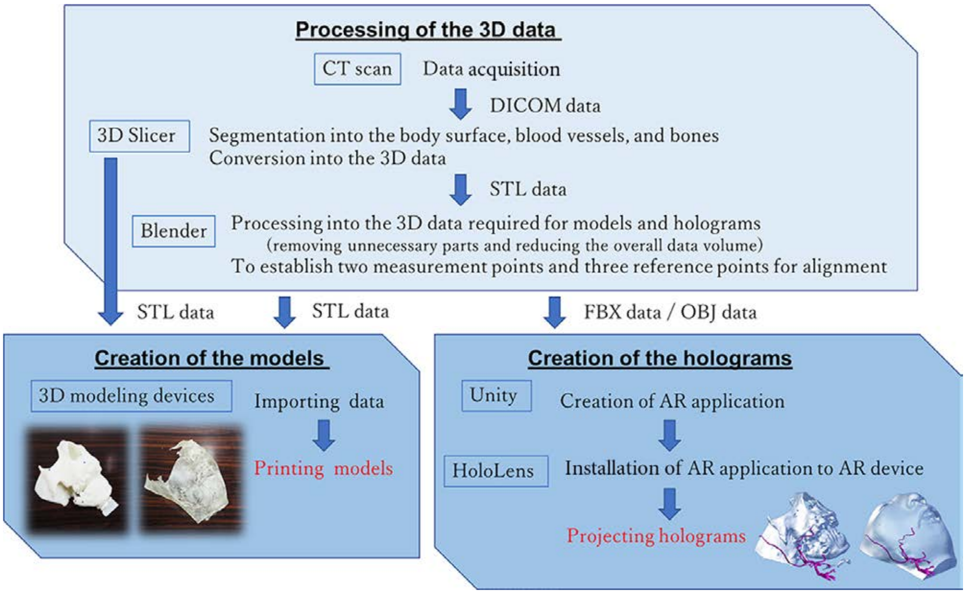

Fig. 1. The workflow for this study. Regarding the production process, both models and holograms require 3D data processing; so the process is the same up to the halfway point. Standard triangulated language (.stl) is one of the file formats used for storing data representing 3D shapes. Filmbox (.fbx) is a popular 3D data interchange format utilized between 3D editors and game engines. Wavefront OBJ (.obj) is a standard 3D image format that can be exported and opened by various 3D image editing programs. The software and engines used were 3D Slicer, a free 3D image analysis software (The Slicer Community, http://www.slicer.org); Blender, a free 3D computer graphics software (Blender Foundation, Amsterdam, the Netherlands, www.blender.org); and Unity, a free game engine (Unity Technologies, Copenhagen, Denmark).

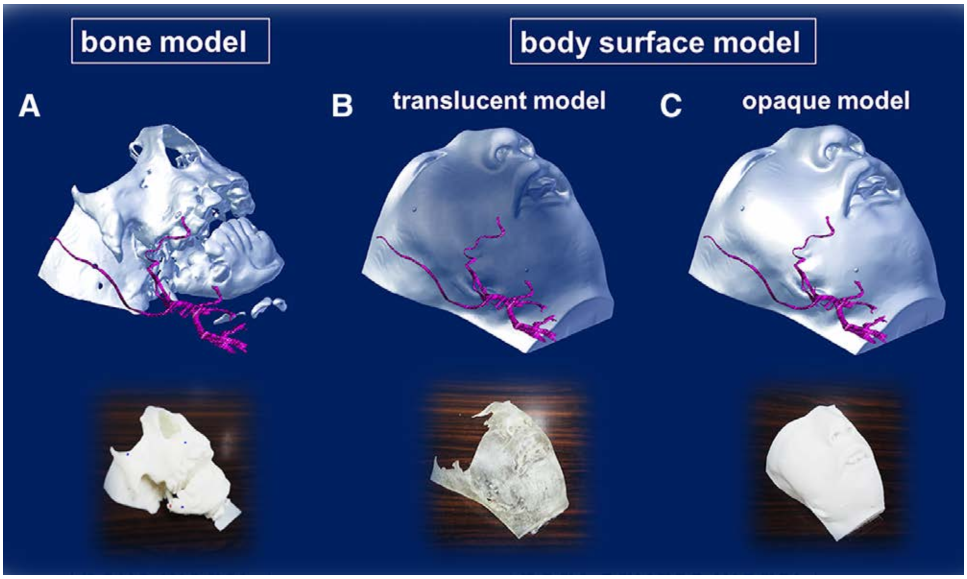

Fig. 2. A, Bone model. B, Translucent body surface model. C, Opaque body surface model. The blood vessel shown is the shallow superficial temporal artery. Images of the models actually used are shown at the bottom of each.

between the two measurement points, point a on the bone surface and point b on the body surface, was then measured in millimeters. The actual distance "ab" between the two measurement points on the computed tomographic scan data was 16.2 mm. Next, the participants observed the hologram overlaid on each model from two different directions relative to the model. The direction approaching the face from the side was designated as the surgical field angle, and that approaching the face from the midline was designated as the midline angle (Fig. 3).

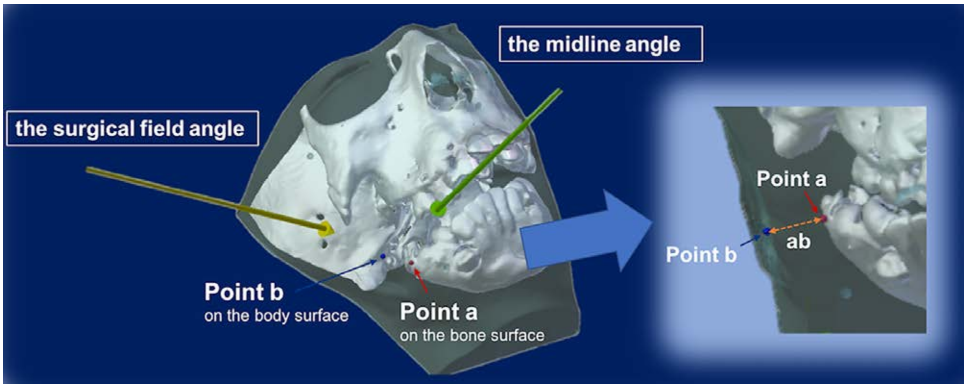

Fig. 3. The measurement points, point a on the bone surface and point b on the body surface, are shown. The distance "ab" between the two points on the computed tomographic scan was 16.2 mm. The direction of observation of the participant is indicated by yellow and green arrows. The direction of the lateral approach to the face is "the surgical field angle," corresponding to the direction of the yellow arrow. The direction of approach from the midline to the face is "the midline angle," corresponding to the direction of the green arrow.

Incidentally, the surgical field angle is close to the field of view in actual surgery, and the depth component of the vector of point a-b is large when viewed from the observation viewpoint. The midline angle is the direction in which the vector direction of the line of sight and that of point a-b are close to perpendicular, and the depth component of the vector of point a-b is small when viewed from the observation viewpoint (Fig. 4). A 1-mm diameter rod was inserted from point b on the body surface, and when the tip reached point a on the bone surface, a point corresponding to point b on the rod was marked. A hole was predrilled at point b on the body surface model for insertion. The distance "a'b'" from the tip (point a') to the marking (point b') was then measured in millimeters (Fig. 5). Two participants familiar with the handling of the equipment performed measurements in a similar manner, with each taking 15 measurements in one direction per model. For each measurement, the application was activated, the holograms were aligned and observed from the specified angle, and measurements were taken. Note that only translucent body surface models were used in experiment 2 because the tips of the measuring rods are not visible on opaque body surface models, making the measurement itself impossible.

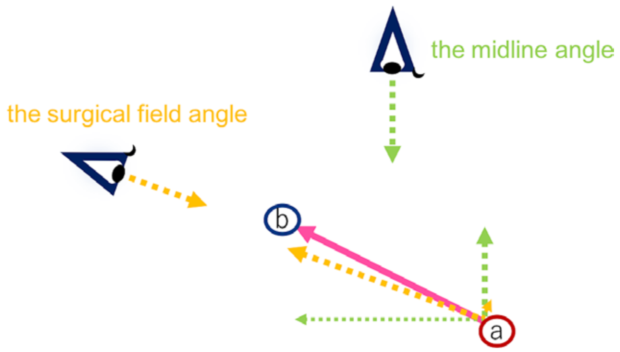

Fig. 4. The distance "ab" between two points is indicated by a pink arrow. When this distance ab is viewed from each observation point, it is divided into a depth component and a horizontal component. Then, the angle at which the depth component of ab increases is the surgical field angle, and the angle at which the depth component of ab decreases is the midline angle.

Statistical Analysis

The measurement error "a'b' – ab" was calculated, and the Wilcoxon signed rank sum test was used to test whether there was a difference in measurement error between the model-hologram-type and angle-type combinations at a 5% risk rate. Statistical analysis was performed using the Statcel4 add-in for Excel Statistics (Nebula Company, Tokyo, Japan).

RESULTS

Experiment 1

The ease of recognizing the vascular holograms in the bone model, the translucent body surface model, and the opaque body surface model differed (Fig. 6). The results showed that the bone model, the translucent body surface model, and the opaque body surface model, in that order, made it easier to understand the positional relationships. Regarding the bone model, seven of the 10 respondents answered "I could recognize it immediately after starting the observation," while for the translucent body surface model, six of the 10 respondents answered "I could recognize it after some time." Regarding the opaque body surface model, four of the 10 respondents answered "I couldn't recognize it."

Experiment 2

The participants had difficulty simultaneously gazing binocularly at one point on the hologram and one point on the measuring rod to be measured, but the measurement error was only about 11.0 mm at most. The median value of the measurement for any combination was 18–20 mm (Fig. 7), which was greater than that for the computed tomographic scan data (16.2 mm).

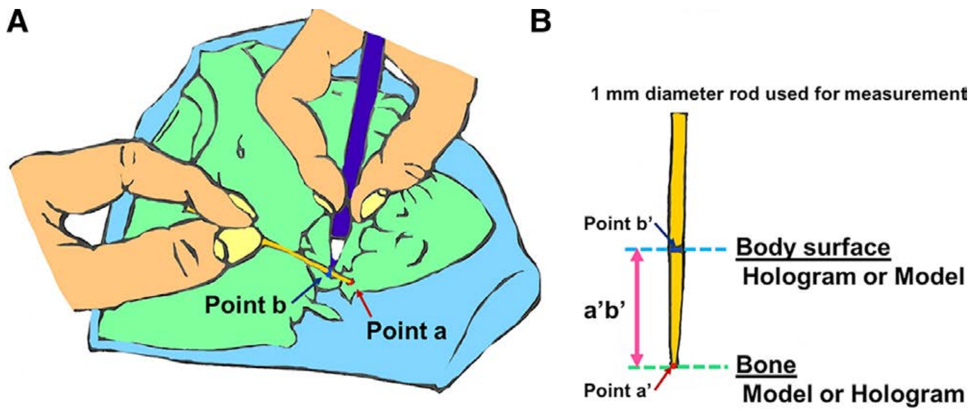

Fig. 5. Actual measurement method. The actual measurement is shown in A. A 1-mm diameter rod is inserted from point b on the body surface, and when the tip reaches point a on the bone surface, a point corresponding to point b on the rod is marked. The distance a'b' from the tip of point a' of the rod to the marking point b' is measured, as shown in B.

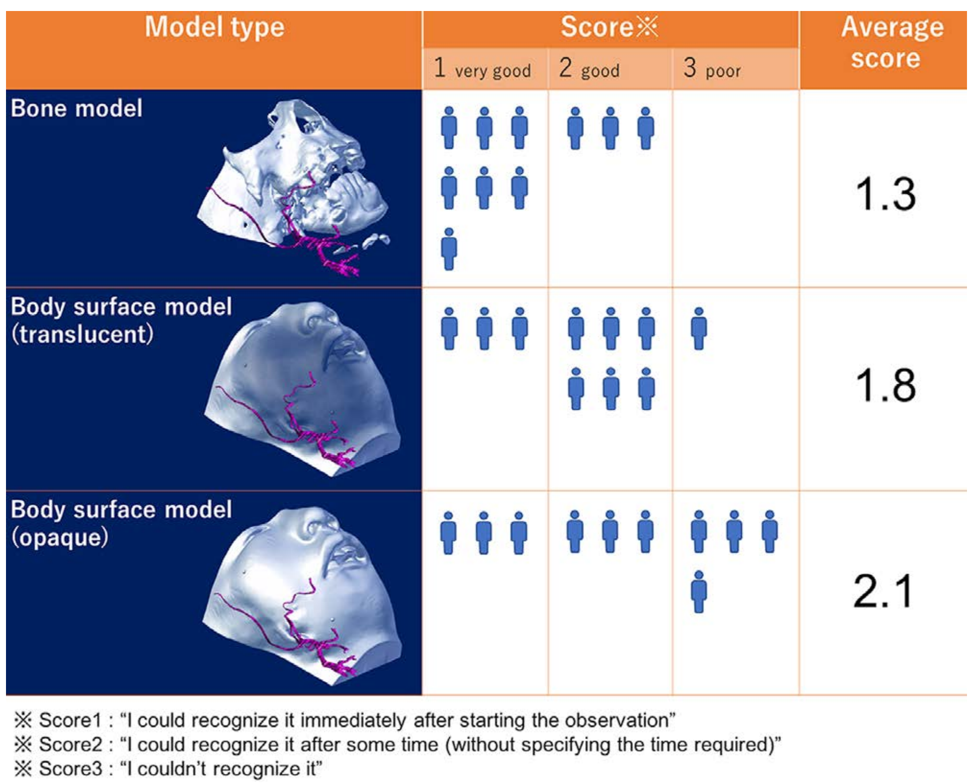

Fig. 6. The following are the results of 10 junior residents' first impressions of the three-dimensional relationship between the holograms of blood vessels and each model—that is, whether they could grasp which was the superficial or deep layer, on a three-point scale. The results showed that the bone model, the translucent body surface model, and the opaque body surface model, in that order, made it easier to understand the positional relationships.

The orange arrows show that differences were seen depending on whether the model or holograms were used for the superficial or deep layers at the same angle (Fig. 7). The measurement error at the surgical field angle was significantly larger for the body surface hologram onto the bone model than for the bone hologram onto the body surface model ($P = 0.01$). In contrast, the measurement error at the midline angle was not significantly different between the body surface hologram onto the bone model and the bone hologram onto the body surface model ($P = 0.73$).

The blue arrows show the difference in measurement by angle using same model-hologram combination (Fig. 7). The measurement error for the body surface

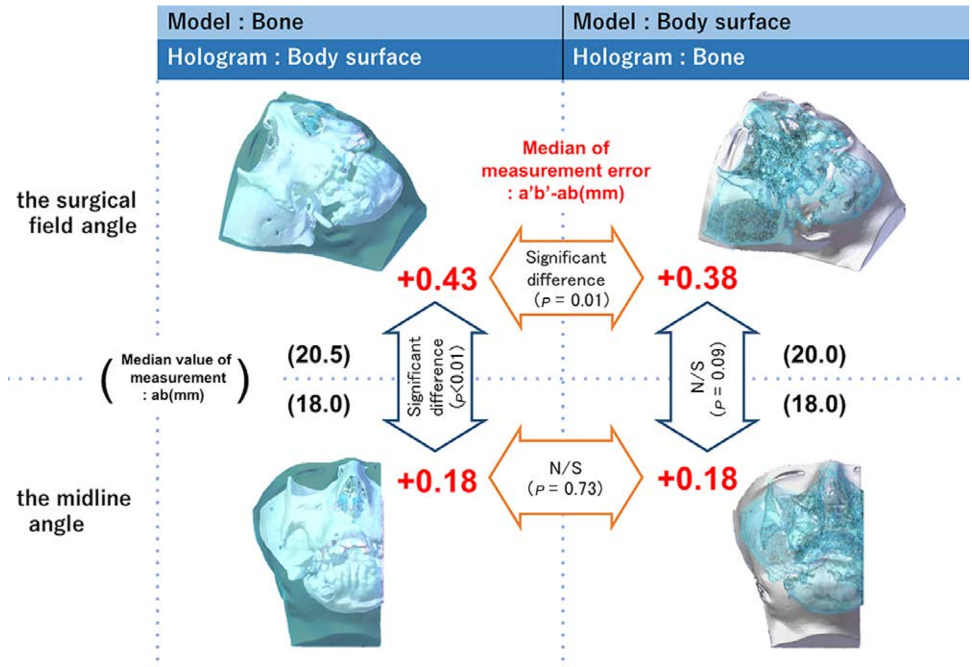

Fig. 7. The top row shows the model-hologram combination, and the left column shows the type of angle. As indicated by the orange arrows, a difference in measurement error was observed depending on whether a model or hologram was used for the superficial or deep layers at the same angle. The measurement error at the surgical field angle was significantly larger for the body surface hologram onto the bone model than for the bone hologram onto the body surface model ($P = 0.01$). In contrast, the measurement error at the midline angle was not significantly different between the body surface hologram onto the bone model and the bone hologram onto the body surface model ($P = 0.73$). On the other hand, the blue arrows indicate that there was a difference in measurement error depending on the angle for the same model and hologram combination. The measurement error for the body surface hologram & bone model was significantly greater for the surgical field angle than for the midline angle ($P < 0.01$). On the other hand, the measurement error for the body surface model & bone hologram did not reach statistical significance ($P = 0.09$), although the measurement error tended to be larger for the surgical field angle.

hologram onto the bone model was significantly greater for the surgical field angle than for the midline angle ($P < 0.01$). On the other hand, the measurement error for the bone hologram onto the body surface model did not reach statistical significance ($P = 0.09$), although the measurement error tended to be larger for the surgical field angle.

Clinical Application

Previous examples of the clinical use of a combination of AR and 3D models are shown in Table 1. A representative case study is provided as follows.

Case 1 is a case of functional temporomandibular joint reconstruction by rib cartilage grafting for micrognathia. When projecting holograms onto a bone model, the positional relationship between a body surface, blood vessels, and bone was easy to understand (Fig. 8A, B). However, in a three-layer body surface model,[20] holograms of blood vessels and bones seemed to float on the surface of the model, and depth could not be reproduced (Fig. 8C).

Cases 3 and 4 are alveolar bone grafts for bilateral cleft lip and palate. In case 3, a bone model was made, and a hologram of the mucosa taken with a 3D imaging system was projected onto the cleft jaw (Fig. 9A). Because it was difficult to see the detailed anatomy in the isometric model, case 4 was improved by using a double-sized bone model and a mucosa hologram (Fig. 9B).

Case 5 is an osteotomy for a bony deformity of the macrodactyly. Using a meshed skin model[21] with a structure that facilitates observation of the interior facilitated the recognition of holograms of blood vessels and bones inside the model and reproduced depth (Fig. 10).

DISCUSSION

Experiment 1

As expected, the combination of projecting a vascular hologram onto a bone model that did not result in a DPP was the most recognizable. When the body surface was opaque, a DPP was generated and recognition was most difficult, but this was improved when the body surface was translucent. This finding suggested that the DPP could be reduced by modifying the model, which is a real object.

Table 1. Representation of Previous Examples of Clinical Use of the Combination of AR and 3D Models

Case	Diagnosis	Age(y)	Gender	Surgical Procedure	Model	AR	Purpose
1	Pierre Robin syndrome	8	Feminine	Functional temporomandibular joint reconstruction	Bone	Body surface Blood vessels	To establish a safe incision line and approach that does not injure the STA†
					Three-layer[20]*	Blood vessels	
2	Binder syndrome	21	Feminine	Rhinoplasty	Three-layer[20]*	Body surface	To evaluate the external nasal morphology before and after surgery
3	Bilateral cleft lip and palate	9	Feminine	Bone graft for alveolar cleft	Bone	Body surface	To educate the resident to understand the anatomy of the mucosa and bone in the cleft
4	Bilateral cleft lip and palate	10	Masculine	Bone graft for alveolar cleft	Bone	Body surface	
					Double-sized bone	Double-sized body surface	
5	Macrodactyly	13	Feminine	Osteotomy for bone deformity	Body surface (translucent)	Blood vessels Bones	To establish a safe incision line and approach that does not injure blood vessels
					Meshed skin[21]‡	Blood vessels Bones	

*The three-layer model represents the body surface, subcutaneous tissue, and bone in a three-layer structure of different materials.
†STA, superficial temporal artery.
‡Meshed skin model is created from three-dimensional data that transforms the body surface layer into a mesh-like structure of about 1 mm thickness.

Experiment 2

Although it was expected from the results of experiment 1 that the measurement error would be small in the bone model and large in the body surface model, the results of experiment 2 were different. In the observation from the surgical viewing angle, the measurement error for the body surface hologram onto the bone model was significantly larger than that for the bone hologram onto the body surface model. We consider the cause of this to be the illusion caused by brightness[22–25] and the effect of the magnitude of the depth vector in the observation direction. An object with high brightness is more likely to be recognized as being in the foreground."[22–25] Holograms should be brighter than the actual landscape to increase visibility. If holograms are projected on the surface layer of the model, the distance between the two points on the superficial hologram and deeper model is likely to seem wider; conversely, if holograms are projected on the layer deeper than the model, the distance between the two points on the deeper hologram and superficial model is likely to seem narrower. Therefore, the error is likely to be magnified in the former case and reduced in the latter (Fig. 11A,B). In addition, the measurement error tends to be larger at the surgical field angle than at the midline angle because the depth component of the vector of point a-b is larger at the surgical field angle (Fig. 4). On the contrary, at the midline angle, the direction of the optical illusion due to the difference in brightness and the measurement direction between points a-b differed significantly, and the depth component of the vector between points a-b was smaller than that at the surgical field angle. For these reasons, it is possible that the measurement error at the midline angle is smaller and not significant (Figs. 4, 12A,B).

In experiment 1, the visibility of the hologram as a first impression differed depending on the type of model. On the other hand, in experiment 2, where the participants actually measured the distance between the two points, the measurement error changed depending on the combination of the model and hologram and the observation viewpoint. However, under either condition, the error was not large enough to cause a misunderstanding of the depth relationship between the surface and deep layers. Therefore, any combination can be used for preoperative examinations and anatomical study purposes. However, because of the variation of a few millimeters, it may be difficult to use as a navigation system in precise operations such as vascular puncture. Also, in HoloLens, the focal distance is fixed at 2m; so no matter what the distance of the hologram is, the observer's crystalline lens will be in the same state as when looking at a real object 2m away. Therefore, if the observer tries to observe the hologram and the real object existing at the same position at the same time, one of them will become unclear and may cause a measurement error.

In the clinical cases, preoperative simulation such as projecting a hologram of the body surface and blood vessels onto a bone model for a bone grafting approach, or designing incision lines and approaches by projecting a hologram of blood vessels and bone onto a meshed skin model[21] was found to be useful.

There have been some reports of improvements in the DPP by devising a display method for virtual objects,[26–29] but to our knowledge, no studies have examined the influence of the real object of the projection destination, as in the present article. In addition, there are no reports regarding the DPP at very shallow depths between the skin and subcutaneous areas, where surgical operations are required mainly in the field of plastic surgery. Projecting holograms onto a deep model (eg, bone models) or considering materials in the case of body surface models, as in this method, is a more desirable method, as it reduces the DPP and improves anatomical understanding. Moreover, when observing positional relationships by projecting a hologram on the model, the DPP may be improved by observing from not only the operator's viewpoint angle, but also multiple other angles. In this case, the angle at which the depth vector component of the observed area becomes smaller is desirable.

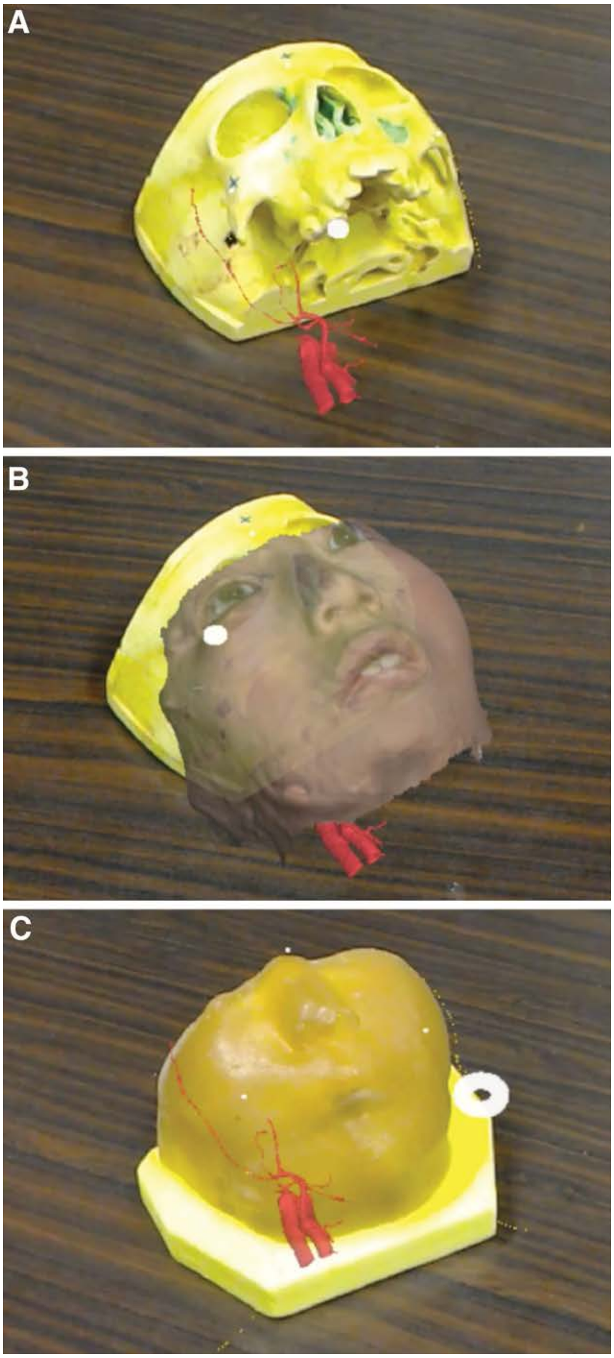

Fig. 8. Preoperative simulation of functional temporomandibular joint reconstruction by rib cartilage grafting was performed for case 1, a patient with micrognathia. A, A hologram of blood vessels was projected onto a bone model. B, A hologram of the body surface was further projected. C, A hologram of a blood vessel was projected onto a three-layer model. It was easier to understand the respective anatomical positions of the body surface, blood vessels, and bones when holograms of blood vessels and the body surface were projected onto the bone model.

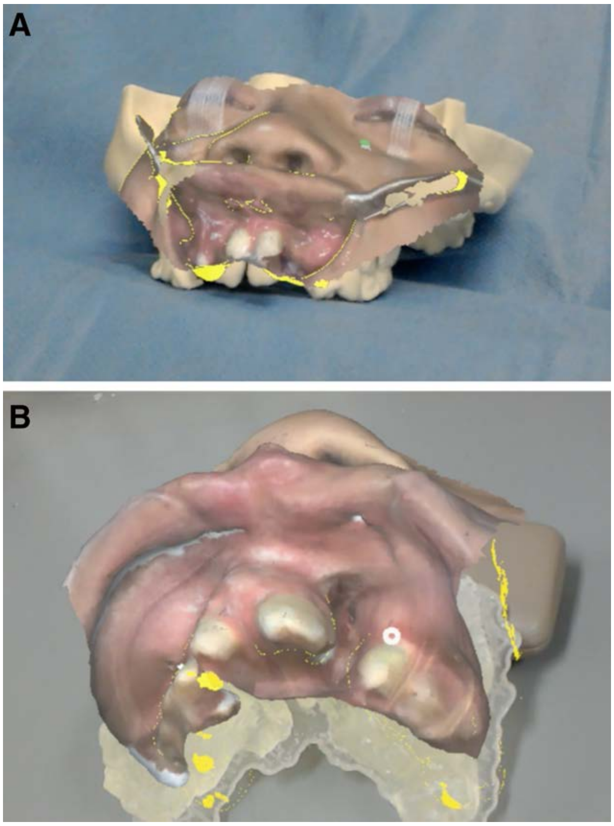

Fig. 9. Cases 3 and 4 are cleft bone grafts for alveolar cleft in bilateral cleft lip and palate. A, In case 3, an isometric bone model was made, and a mucosal hologram taken using a 3D imaging system was projected onto the cleft jaw. B, Because the detailed anatomy was not clear, case 4 was improved by using a double-sized bone model and mucosa hologram.

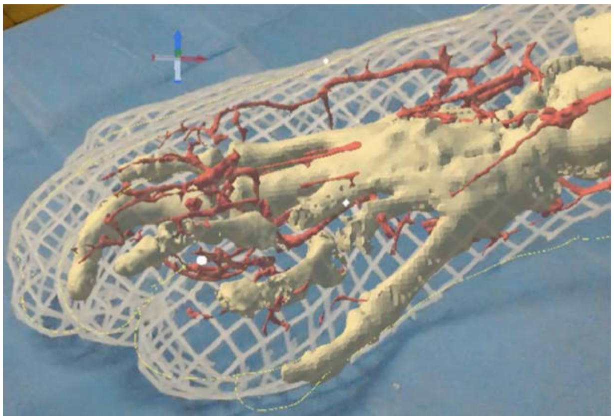

Fig. 10. In case 5, a preoperative simulation was performed to study the surgical approach to osteotomy for a bony deformity of the macrodactyly. The use of a meshed skin model facilitated the recognition of blood vessels and bone inside the model and reproduced depth. In addition, incision lines could be designed on the surface of the model.

In this study, we investigated the relationship between the body surface layer/bone layer and the running of specific blood vessels. There is also room for evaluation of the

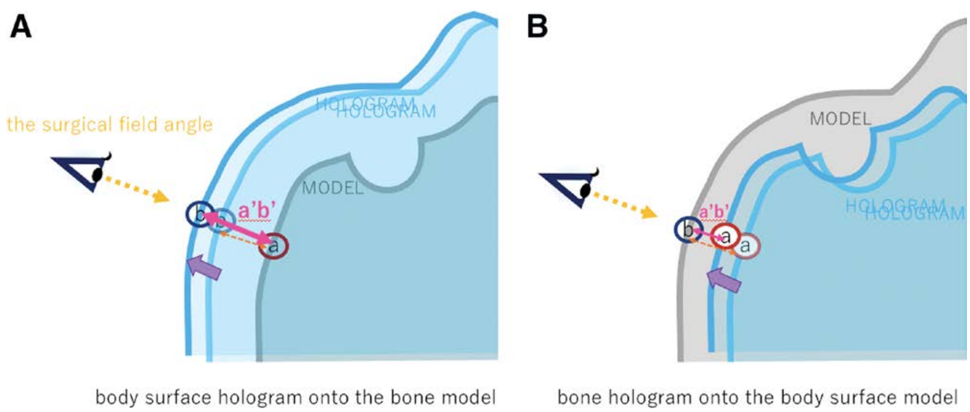

Fig. 11. Each combination of the model and the hologram at the surgical field angle where the depth vector is large. Gray objects indicate models and light blue objects indicate holograms. The purple arrows indicate the direction of the illusion in which the hologram appears more in the foreground because of the difference in brightness created. Difference in the effects of illusions could explain the difference in statistical results. A, Due to this illusion, it is probable that a'b' was perceived to be further apart in the body surface hologram onto the bone model. B, Due to this illusion, it is probable that a'b' was perceived to be closer in the bone hologram onto body surface model.

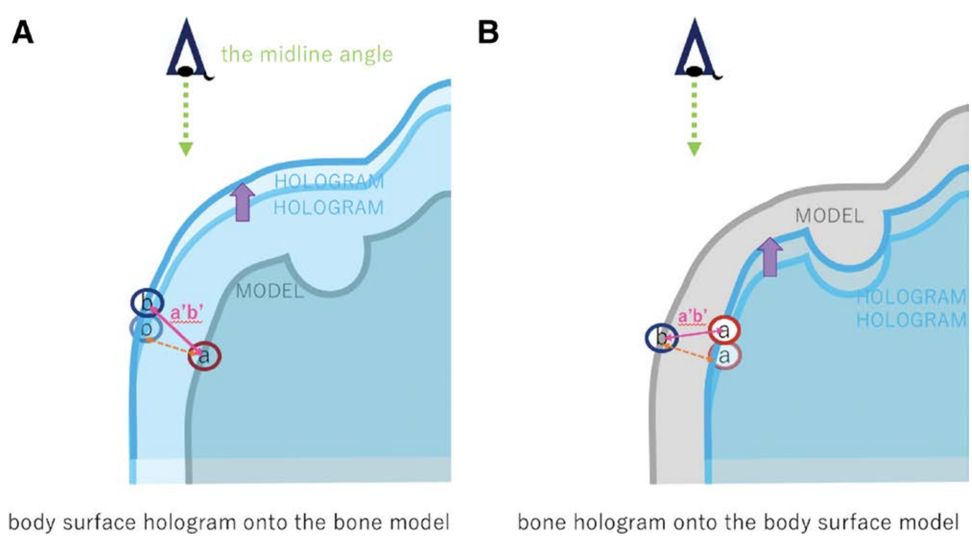

Fig. 12. Each combination of the model and the hologram at the midline angle is shown. The direction of the illusion caused by the difference in brightness and the direction of the measurement of the distance ab between two points are very different in both combinations. Therefore, it is unlikely that the difference as in the case of the surgical field angle in Figure 11 is generated. A, body surface hologram onto the bone model. B, bone hologram onto body surface model.

relationship with the intermediate layer such as SMAS and muscle layer. Considering the limitations of AR technology, we would like to further explore how it can be more effectively incorporated into the surgical field.

CONCLUSIONS

In this article, two experiments investigated how to effectively project holograms onto a 3D model. The results indicated that the impression of the positional relationship and the actual measurement results differed depending on the combination of model and hologram types. In the context of our experience with clinical cases, these findings suggest that the DPP could be improved by changing the combination of the model and hologram, the material of the model, and the observation angle.

Daisuke Mitsuno, MD, PhD
Department of Plastic and Reconstructive Surgery
Osaka Medical and Pharmaceutical University
2-7 Daigaku-cho, Takatsuki City
Osaka 569-8686, Japan
E-mail: daisuke.mitsuno@ompu.ac.jp

DISCLOSURE

The authors have no financial interest to declare in relation to the content of this article.

ACKNOWLEDGMENTS

The authors did not describe experimental studies on humans or animals. They have no ethical approval of studies and informed consent in relation to the content of this article.

REFERENCES

1. Azuma RT. A survey of augmented reality. *Presence Teleop Virt*. 1997;6:355–385.
2. Sutherland J, Belec J, Sheikh A, et al. Applying modern virtual and augmented reality technologies to medical images and models. *J Digit Imaging*. 2019;32:38–53.
3. Wang J, Suenaga H, Yang L, et al. Video see-through augmented reality for oral and maxillofacial surgery. *Int J Med Robot*. 2017;13:e1754.
4. Carl B, Bopp M, Saß B, et al. Implementation of augmented reality support in spine surgery. *Eur Spine J*. 2019;28:1697–1711.
5. Tarutani K, Takaki H, Igeta M, et al. Development and accuracy evaluation of augmented reality-based patient positioning system in radiotherapy: a phantom study. *In Vivo*. 2021;35: 2081–2087.
6. Alice I, Giglioli C, Pallavicini F, et al. Augumented reality: a brand new challenge for the assessment and treatment of psychological disorders. *Comput Math Methods Med*. 2015;862942:12.
7. Rüger C, Feufel MA, Moosburner S, et al. Ultrasound in augmented reality: a mixed-methods evaluation of head-mounted displays in image-guided interventions. *Int J Comput Assist Radiol Surg*. 2020;15:1895–1905.
8. Rodrigues TB, Catháin CO, O'Connor NE, et al. A quality of experience assessment of haptic and augmented reality feedback modalities in a gait analysis system. *PLoS One*. 2020;15:e0230570.
9. Mitsuno D, Hirota Y, Akamatsu J, et al. Telementoring demonstration in craniofacial surgery with hololens, skype, and three-layer facial models. *J Ctaniofac Surg*. 2019;30:28–32.
10. Shenai MB, Tubbs RS, Guthrie BL, et al. Virtual interactive presence for real-time, long-distance surgical collaboration during complex microsurgical produres. *J Neurosurgery*. 2014;121:1–8.
11. Ma M, Fallavollita P, Seelbach I, et al. Personalized augmented reality for anatomy education. *Clin Anat*. 2016;29:446–453.
12. Bork F, Stratmann L, Enssle S, et al. The benefits of an augmented reality magic mirror system for integrated radiology teaching in gross anatomy. *Anat Sci Educ*. 2019;12:585–598.
13. Mitsuno D, Ueda K, Itamiya T, et al. Intraoperative evaluation of body surface improvement by an augmented reality system that a clinician can modify. *Plast Reconstr Surg Glob Open*. 2017;5:e1432.
14. Umeda C, Ueda K, Mitsuno D, et al. Collaboration of AR device and separable two-layered elastic models as tools for surgical education. *Plast Reconstr Surg. Glob Open*. 2022;10:e4182.
15. Uehira K, Suzuki M. Depth perception for virtual object displayed in optical see-through HMD. ACHI. *The Eleventh International Conference on Advances in Computer-Human Interactions*. 2018:204–205.
16. Armbrüster C, Wolter M, Kuhlen T, et al. Depth perception in virtual reality:distance estimations in peri- and extrapersonal space. *Cyberpsychol Behav*. 2008;11:9–15.
17. Martin GA, Weiss J, Keller A, et al. The impact of focus and context visualization techniques on depth perception in optical see-through head-mounted displays. *IEEE Trans Vis Comput Graph*. 2021;1:1–1.
18. Choi H, Cho B, Masamune K, et al. An effective visualization technique for depth perception in augmented reality-based surgical navigation. *Int J Med Robot*. 2016;12:62–72.
19. Mitsuno D, Ueda K, Hirota Y, et al. Effective application of mixed reality device HoloLens: simple manual alignment of surgical field and holograms. *Plast Reconstr Surg*. 2019;143:647–651.
20. Ueda K, Kino H, Katayama M, et al. Simulation surgery using 3D 3-layer models for congenital anomaly. *Plast Reconstr Surg. Glob Open*. 2020;8:e3072.
21. Mitsuno D, Ueda K, Nuri T, et al. Clinical applications of meshed multilayered anatomical models by low-cost three-dimensional printer. *Plast Reconstr Surg*. 2021;148:1047e–1051e.
22. Cutting JE, Vishton PM. Perceiving layout and knowing distances: the integration, relative potency, and contextual use of different information about depth. *Perception of Space and Motion. Chap.3*. London: Academic Press; 1995:69–117.
23. Scaccia M, Langer MS. Signs of depth-luminance covariance in 3-D cluttered scenes. *J Vis*. 2018;18:5.
24. Ping J, Thomas BH, Baumeister J, et al. Effects of shading model and opacity on depth perception in optical see-through augmented reality. *J Soc Inf Display*. 2020;28:892–904.
25. Jamiy FE, Marsh R. Survey on depth perception in head mounted displays: distance estimation in virtual reality, augmented reality, and mixed reality. *IET Image Process*. 2019;13:707–712.
26. Katayama M, Ueda K, Mitsuno D, et al. Intraoperative 3-dimensional projection of blood vessels on body surface using an augmented reality system. *Plast Reconstr Surg. Glob Open*. 2020;8:e3028.
27. Bichlmeier C, Nvab N. Virtual window for improved depth perception in medical AR. In: International workshop on augmented environments for medical imaging including augmented reality in computer-aided surgery (AMI-ARCS). Copenhagen, Denmark, October 1–6, 2006.
28. Marques B, Haouchine N, Plantefeve R, Cotin S. Improving depth perception during surgical augmented reality. ACM SIGGRAPH 2015 Posters. Aug, 2015; Los Angeles, United States.
29. Lerotic M, Chung AJ, Mylonas G, et al. Pq-space based non-photorealistic rendering for augmented reality. *Med Image Comput Assist Interv*. 2007;10:102–109.